20 minutes and blocked with universal blocking agent. Immunofluorescent ICAM-1 staining was carried out by incubating the cardiomyocytes with 1:500 mouse anti-rat ICAM-1 antibody (BD Biosciences) followed by Alexa Fluor 594-labeled goat anti-mouse antibody. The cardiomyocytes were examined using a confocal microscope (Leica) as described in the previous section. The scan format was 1,024 × 1,024 pixels, and 2× zoom was applied.

Statistical analysis

All data are expressed as mean ± standard error. For each experimental condition and time point, at least four independent replicate analyses were performed, unless otherwise noted. Differences between groups were tested using a one-way analysis of variance and the *post hoc* Bonferroni test to identify specific differences between groups. Differences were considered significant for P values of less than 0.05.

Results

Systemic inflammation depresses cardiac contractility and is associated with intracardiac extravasation of fibrinogen and increased expression of ICAM-1 by cardiomyocytes

We determined whether endotoxin would create an environment within the heart which would allow ICAM-1 expressed on cardiomyocytes to interact with extravasated fibrinogen and whether this would be associated with alterations in cardiac contractility. Six hours after LPS injection, the endotoxemic group of rats exhibited decreased left ventricular contractility compared with the saline-treated controls (Figure 1). Cardiac cycle pressure-volume loops using mean data clearly demonstrate an LPS-induced rightward shift along the volume axis. This shift reflects left ventricular dilation represented by increased EDV, maintenance of stroke volume (SV), and resultant marked reduction of left ventricular EF (EF = SV/EDV) (Figure 1 and Table 1). The preload-independent E_{max} is dramatically decreased in LPS-treated versus saline-treated rats, whereas (dP/dT)/EDV reflects isovolemic contractility and is also depressed with LPS (Table 1). Immunostaining of heart tissue from these rats demonstrated a dramatic increase in both intramyocardial ICAM-1 expression and perivascular fibrinogen in the myocardium of LPS-treated rats (Figure 2a,b). Image quantification demonstrated a 5.5 ± 1.6-fold increase in ICAM-1 expression and a 2.1 ± 0.6-fold increase in perivascular fibrinogen in the myocardium of LPS-treated rats (Figure 2c).

ICAM-1 expressed on activated isolated cardiomyocytes specifically binds to fibrinogen

By means of confocal microscopy, ICAM-1 was found to be present on the cell surface of TNF-α-activated cardiomyocytes. Co-immunostaining with fluorescently labeled fibrinogen demonstrated a high degree of colocalization (Figure 3a), supporting previous reports of interaction between these two molecules [17,21]. To confirm that fibrinogen specifically bound ICAM-1, we pre-treated isolated cardiomyocytes with either with an ICAM-1-blocking antibody or non-specific IgG. Compared with the IgG control group, cardiomyocytes treated with blocking antibody to ICAM-1 exhibited significantly lower adherence to fibrinogen-coated beads (Figure 3b). ICAM-1 is known to interact with fibrinogen via ICAM-1 peptides 8–22. To confirm this specific interaction between ICAM-1 and fibrinogen, we performed an ELISA binding assay using immobilized fibrinogen incubated with biotinylated ICAM-1 (8–22) peptide. In dose-finding experiments, as expected with receptor-ligand binding, there is a dose-response curve that reaches saturation at a fibrinogen concentration of 100 μM (Figure 4a). When group mean absorbance data are taken at this plateau fibrinogen concentration of 100 μM, there is a large increase in ICAM-1 (8–22) peptide binding with fibrinogen compared with scrambled peptide (Figure 4b). Thus, fibrinogen specifically binds to ICAM-1 through interaction with ICAM-1 peptides 8–22.

Fibrinogen mediates decreased cardiomyocyte contractility via an ICAM-1-dependent mechanism

We next examined whether ICAM-1 ligation by fibrinogen alters cardiomyocyte contractility. In one series of experiments, isolated cardiomyocytes were pre-treated with either ICAM-1-blocking antibody or isotype control antibody before adding fibrinogen-coated polystyrene beads. Whereas cardiomyocytes pre-treated with isotype control antibody demonstrated a dose-dependent decrease in contractility upon exposure to fibrinogen-coated beads, cardiomyocytes pre-treated with ICAM-1-blocking antibody demonstrated no reduction in contractility (Figure 5). To verify that this interaction is mediated

Table 1

Hemodynamic data from endotoxemic and control animals

Treatment	Heart rate (beats per minute)	Systolic pressure (mm Hg)	Ejection fraction (percentage)	(dP/dT)/EDV	E_{max}
LPS	392 ± 152	108 ± 8	38 ± 2	44 ± 3	2.5 ± 0.4
Control[a]	313 ± 30	112 ± 6	52 ± 8	121 ± 11	7.7 ± 0.6
	P = NS	P = NS	$P < 0.05$	$P < 0.05$	$P < 0.05$

[a]Saline-treated rats. dP, derivative of pressure; dT, derivative of time; EDV, end diastolic volume; E_{max}, maximal end-systolic elastance; LPS, lipopolysaccharide-treated rats; NS, not significant.

Figure 1

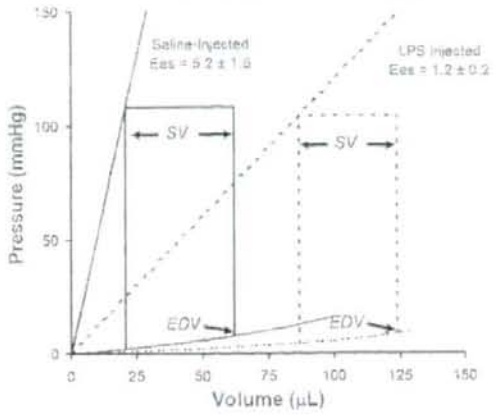

LPS decreases cardiac contractility. Cardiac cycle preasure-volume loops obtained 6 hours after intraperitoneal injection of lipopolysaccharide (LPS) or saline into rats. Acquired with group mean data, the curves demonstrate an LPS-induced increased end diastolic volume (EDV), maintenance of stroke volume (SV), and therefore a marked reduction of left ventricular ejection fraction (SV/EDV). E_{es}, end-systolic elastance.

specifically via the ICAM-1 (8–22) fibrinogen binding site, we performed a competitive assay in which a peptide containing the ICAM-1 (8–22) fibrinogen binding site was pre-incubated with soluble fibrinogen before addition of this mixture to activated isolated cardiomyocytes. Pre-incubation of the fibrinogen with excess ICAM-1 (8–22) peptide abolished the fibrinogen-mediated decrease in cardiomyocyte contractility, whereas pre-incubation of fibrinogen with a 'scrambled' peptide containing the same residues showed no such effect (Figure 6).

Fibrinogen chain D mediates decreased cardiomyocyte contractility

Fibrinogen is composed of three major subunits, a central E chain linked to two D chains (Figure 7a). The smaller gamma chain is always found associated with the D chain and thus is not generally considered to be a distinct subunit. To determine whether the fibrinogen-mediated contractile dysfunction results from interaction of ICAM-1 with the intact whole molecule or whether a single chain contains the binding site, cardiomyocytes were incubated with whole fibrinogen, fibrinogen chain D, or fibrinogen chain E. There was a significant decrease in cardiomyocyte contractility following incubation with whole fibrinogen and fibrinogen chain D, but no effect was seen with fibrinogen chain E (Figure 7b).

Figure 2

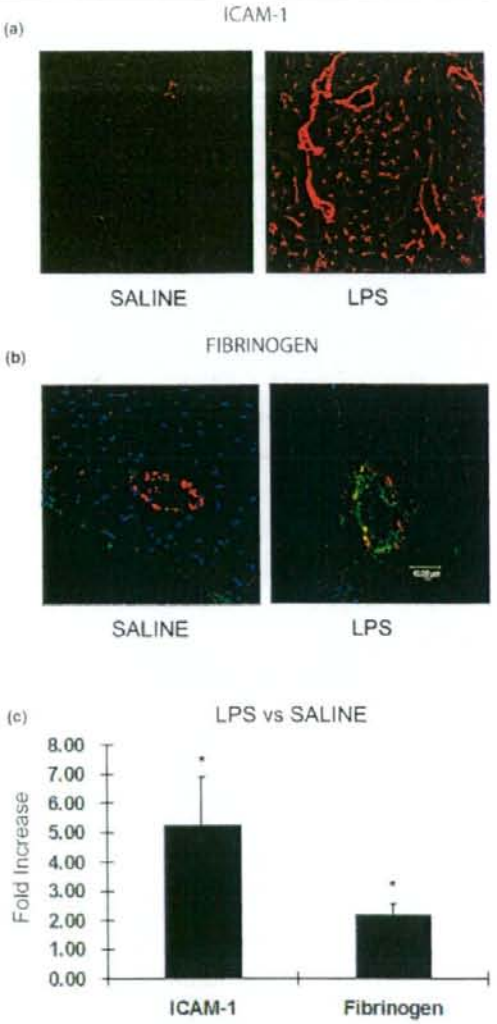

LPS increases intracardiac ICAM-1 and perivascular fibrinogen. (a) Frozen cardiac sections from lipopolysaccharide (LPS)-treated and saline-treated rats demonstrate that intracardiac intracellular adhesion molecule-1 (ICAM-1) (red) is dramatically increased in the former. (b) Fibrinogen (green) was greatly increased outside the endothelium (von Willebrand factor labeled red) in the LPS group compared with rats treated with saline. (c) Group mean data of the fold increases in myocardial ICAM-1 expression and perivascular fibrinogen deposition in LPS-treated versus saline-treated animals. *$p < 0.05$ versus saline.

Figure 3

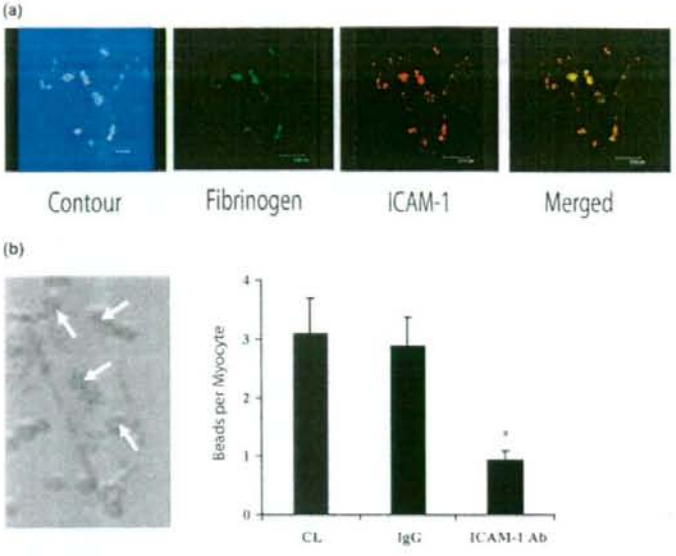

Fibrinogen binds specifically to cardiomyocyte ICAM-1. Colocalization of fibrinogen and cardiomyocyte intracellular adhesion molecule-1 (ICAM-1). **(a)** Isolated cardiomyocytes were incubated with Oregon Green-labeled fibrinogen (green) and fluorescently stained for ICAM-1 (red). A multi-photon dual-excitation image of the contour of the cell of interest is shown. By means of an overlay of images, strong colocalization of fibrinogen and ICAM-1 was indicated by a yellow color. **(b)** A representative image of a rat cardiomyocyte with adherent fibrinogen-coated polystyrene beads (white arrows) is shown to the left of the graph. The specificity of the ICAM-1-fibrinogen interaction is demonstrated as anti-ICAM-1 antibody pre-treatment results in significantly less fibrinogen-coated polystyrene beads adherent to the cardiomyocytes (*$p < 0.05$ versus control). Ab, antibody; CL, control; IgG, immunoglobulin G.

Amino acid sequence 117–133 of the fibrinogen gamma chain is the active site, and the crosslinked gamma chains of D-dimer retain the ability to interact with ICAM-1

We next determined whether the ICAM-1 binding gamma chain site 117–133 [17] of the D chain (Figure 8a) was responsible for the observed contractile dysfunction. Furthermore, as dimerization of fibrinogen chain D (commonly known as D-dimer) is accomplished in part via crosslinking the XL sites of the gamma chain (Figure 8a,b) [27], we tested whether dimerization resulted in attenuation of the ICAM-1-mediated effect. The gamma peptide 117–133 resulted in a significant reduction in fractional shortening compared with control, whereas scrambled peptide had no effect (Figure 8c). Incubation with D-dimer also resulted in a significant reduction in fractional shortening (Figure 8c), demonstrating that the functional site 117–133 remains active despite crosslinking of gamma chains.

Discussion

In this study, we propose a novel mechanism linking two phenomena that occur as a result of inflammation: dysregulation of the coagulation cascade and myocardial dysfunction. The key finding reported is that amino acid sequence 117–133 of the fibrinogen gamma chain decreases cardiomyocyte contractility through binding ICAM-1. Of great interest to clinicians is that D-dimer, a product of fibrinogen polymerization and subsequent digestion which includes 117–133 of the gamma chain, in addition to its important role in diagnosis of thromboembolism, can decrease cardiomyocyte contractility.

It has long been recognized that seemingly disparate causes of local or systemic inflammation, such as ischemia reperfusion, inflammatory cardiomyopathy, orthotopic heart transplant rejection, or sepsis [1-3], all culminate in myocardial dysfunction. While each disorder undoubtedly poses unique challenges to the maintenance of myocardial homeostasis, there could be a factor that is common to all. Endothelial damage with subsequent capillary leakage represents a final common pathway of inflammatory disorders [28]. Increased permeability of the endothelium leads to a shift of circulating elements from the plasma into the organs. Should this fluid flux contain circulating substances capable of depressing myocardial contractility, this may be the link between myocardial dysfunction and inflammatory states. This depressant not only must reach the cardiac myocytes but must have a receptor capable of mediating changes in contractility. We have previ-

Figure 4

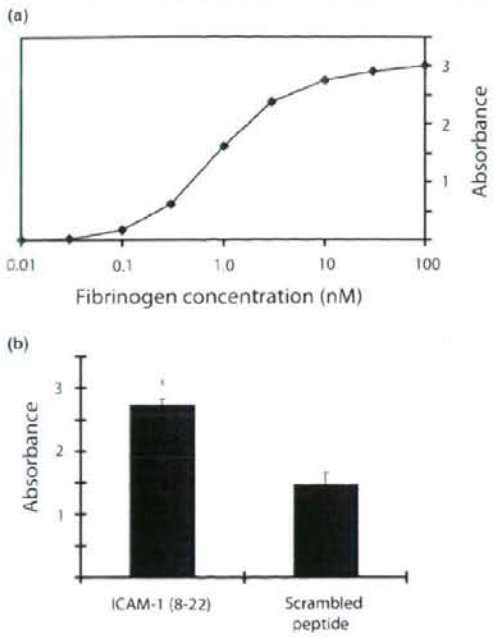

ICAM-1 (8–22) binds to fibrinogen. Two-step enzyme-linked immunosorbent assay in which fibrinogen was immobilized on the 96-well plate and then incubated with biotinylated intracellular adhesion molecule-1 (ICAM-1) (8–22) peptide or biotinylated 'scrambled' control peptide. Anti-biotin antibody was added, and colorimetric absorbance quantified the peptide-fibrinogen interaction. **(a)** Representative ICAM-1 (8–22) dose-response curve showing absorbance plateau at a fibrinogen concentration of approximately 100 μM. **(b)** Group mean absorbance data taken at the plateau fibrinogen concentration (100 μM) demonstrating a strong interaction between the ICAM-1 (8–22) peptide and fibrinogen compared with a small non-specific interaction between the scrambled peptide and fibrinogen. *$p < 0.05$ versus scrambled peptide.

ously shown that ICAM-1 expressed on cardiomyocytes is induced by inflammatory mediators and, upon activation, is capable of decreasing cardiomyocyte contractility [9,13].

Any circulating ICAM-1 ligands could be candidates for causing myocardial dysfunction provided that they permeate the heart. CD11a/CD18 (LFA-1) and Cd11b/CD18 (Mac-1) expressed on the surface of polymorphonuclear leukocytes are ICAM-1 ligands capable of reducing myocyte contractility *in vitro* [11] and have been proposed to be the link between inflammation and cardiac dysfunction. However, we and others have noted a striking paucity of intramyocardial leukocytes in whole animal models of inflammation [12,13]. Fibrinogen, as well as its related protein fragments D-dimer and other FDPs, represents potential ICAM-1 binding myocardial depressant substances. Through both human epidemiologic data and

Figure 5

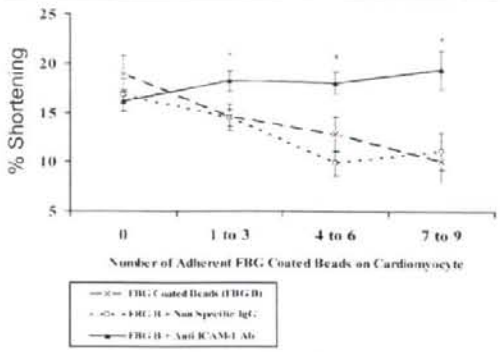

Fibrinogen decreases cardiomyocyte fractional shortening via ICAM-1. Cardiomyocytes were pre-treated with either a blocking anti-ICAM-1 antibody or isotype control antibody prior to the addition of fibrinogen-coated beads. Fractional shortening was then measured. Whereas pre-treatment with immunoglobulin G (IgG) isotype antibody was no different than fibrinogen alone, treatment with blocking anti-ICAM-1 antibody prevented the fibrinogen-induced decrease in fractional shortening. *$p < 0.05$ versus fibrinogen beads alone. Ab, antibody; FBG, fibrinogen; ICAM-1, intracellular adhesion molecule-1.

basic science, fibrinogen and FDPs satisfy two major criteria for causality. Clinically, not only are fibrinogen and D-dimer markedly increased in inflammatory disorders, but their levels are inversely correlated with favorable outcome [4-8]. As for biologic plausibility, the amino acid sequence 117–133 of fibrinogen gamma chain (fg-γ-117–133) is capable of binding the amino acid sequence 8–22 (ICAM-1-8–22) within the first Ig domain of ICAM-1 [17]. While the fibrinogen-ICAM-1 interaction facilitates adhesion of leukocytes to endothelial cells [18,19], leukocyte transmigration [20], and promotion of endothelial cell survival [21], there is no information regarding its role in cardiac physiology.

In this study, we show for the first time that fibrinogen is capable of mediating a reduction in cardiomyocyte contractility thorough activation of ICAM-1. It is important to note that significant reduction in fractional shortening was achieved at a fibrinogen concentration of 0.2 mg/mL, approximately one order of magnitude less than its physiological concentration in plasma [27]. Fibrinogen is a large 340-kDa plasma glycoprotein and, as such, would be expected to have limited tissue penetration compared with smaller plasma proteins. Despite its large size, however, we showed a significant increase in perivascular fibrinogen deposition in an *in vivo* model of systemic inflammation. FDPs, notably fragment D (100 kDa) or D-dimer at roughly double that size [27], could potentially infiltrate deeper into the myocardium and exert their depressant effect in areas that fibrinogen could not access. Importantly, not only did we find that systemic injury increased intracardiac fibrinogen, there was a dramatic increase in ICAM-1 expres-

Figure 6

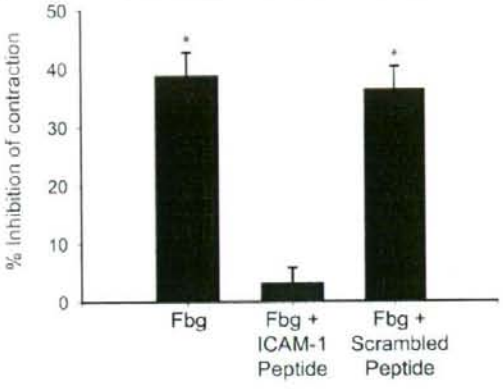

ICAM-1 (8–22) mediates decreased contractility. Before fibrinogen was added to activated cardiomyocytes, soluble intracellular adhesion molecule-1 (ICAM-1) (8–22) peptide, which binds fibrinogen at peptides 117–133, is added in excess to the fibrinogen. Activated cardiomyocytes incubated with fibrinogen alone demonstrate a 40% reduction in contractility. Pre-incubation of fibrinogen with the ICAM-1 (8–22) peptide results in competition between cardiomyocyte-expressed ICAM-1 and the ICAM-1 (8–22) peptide for the fibrinogen active site (117–133). Pre-incubation with the ICAM-1 (8–22) peptide abolishes the reduced contractility seen with fibrinogen alone, whereas pre-incubation with 'scrambled' ICAM-1 peptide had no effect. *$p <$ 0.05 versus control. Fbg, fibrinogen.

Figure 7

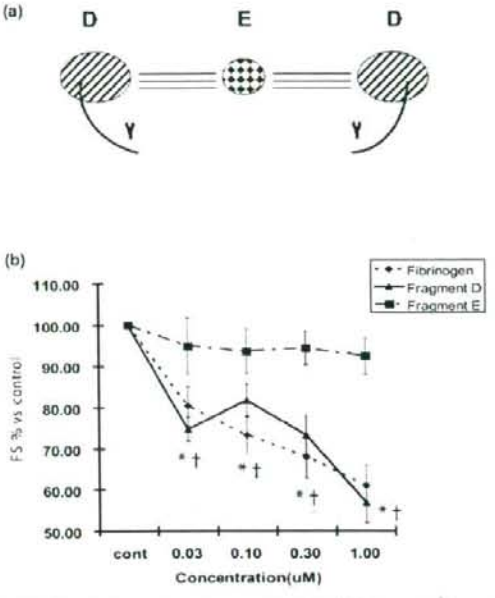

Fibrinogen subunit D decreases contractility. (a) Schematic diagram of the fibrinogen molecule, showing two D chains each containing a gamma chain linked to a central E chain. **(b)** Cardiomyocytes were incubated with whole fibrinogen as well as the major subunits D and E of fibrinogen. Whole fibrinogen and subunit D resulted in significant decreases in fractional shortening (FS), whereas subunit E had no significant effect. *,†$p < 0.05$ versus control.

sion. Thus, our animal models of disease provide *in vivo* evidence to support the hypothesis that fibrinogen and FDPs might be the circulating myocardial depressant factors.

Determining whether the previously identified interaction between fibrinogen and ICAM-1 [17-21] is responsible for alterations in cardiac physiology is fundamental information required both to understand the mechanism and to design potential therapeutics. Fibrinogen consists of two major chains, E and D, as illustrated in Figure 7a. The gamma chain is a subunit of chain D, as shown in Figures 7a and 8a, and contains a crosslinking (XL) site through which two D chains dimerize. The putative active site of fibrinogen is 117–133 on the gamma chain [17] and, though remote from the XL site as shown in Figure 8b, might be altered or allosterically interfered with upon dimerization. We show that fibrinogen chain D causes cardiomyocyte contractile dysfunction whereas chain E had no biologic effect. This agrees with findings by other investigators that it is the D chain responsible for ICAM-1-mediated vasoconstriction [29]. Furthermore, we went on to show that previously identified [17] site 117–133 of the fibrinogen gamma chain was responsible for the ICAM-1-mediated physiologic effects. As the gamma chain is linked to the D chain, it is important to consider it in the context of polymerized D chains. Despite its crosslinked gamma chains, D-dimer also caused significant reductions in contractility. Although the specificity of interaction of D-dimer with fibrinogen was not tested through antibody blockade or competing peptide, we believe that, as it is composed of two D subunits, the mechanism of action is nearly certainly analogous to the individual D chain. This last finding is particularly exciting given that, while long touted as a biomarker for both the presence and prognosis of inflammatory disease [4-8], D-dimer has been perceived, to date, as a disease marker with no intrinsic biologic effect. Not only do we now know that vascular tone can be altered by the fibrinogen D chain's activation of ICAM-1 [29], but here we demonstrate that the key contractile function of cardiac muscle cells is impaired via the same mechanism.

Conclusion

Site 117–133 of the fibrinogen gamma chain is able to depress cardiomyocyte contractility through binding ICAM-1. The implication of the reported mechanism extends beyond the realm of our models of inflammation to other pathologies characterized by inflammation and heart failure, such as post-ischemia reperfusion injury, inflammatory cardiomyopathy, and orthotopic heart transplant rejection.

Figure 8

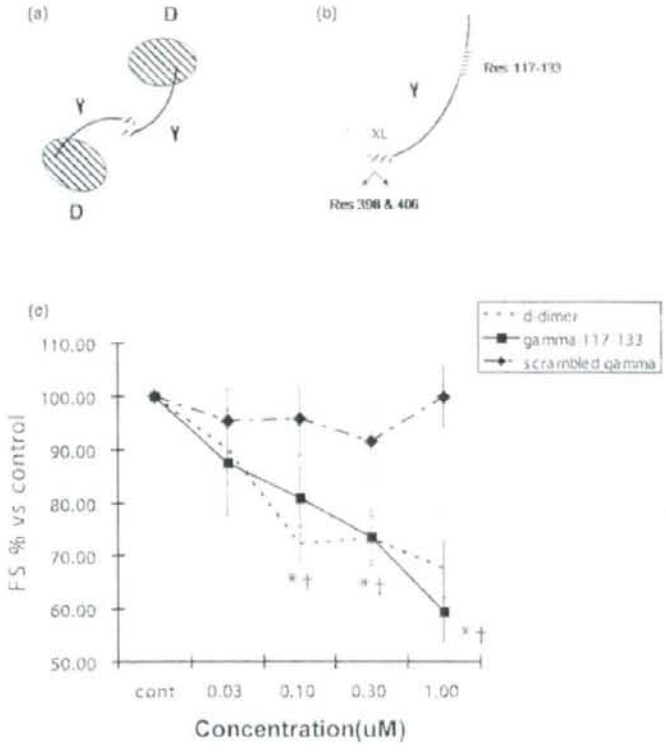

Fibrinogen gamma chain and D-dimer decrease contractility. (a) Schematic diagram of D-dimer with two D subunits linked in part via interaction of the gamma chains. For simplicity, we have not shown the areas on the D chain itself which participate in dimerization. (b) Expanded diagram of the gamma subunit showing the crosslinking (XL) site of the C-terminal regions which results in amine donor lysine 406 of one gamma chain and a glutamine acceptor at residue 398 or 399. The intracellular adhesion molecule-1 (ICAM-1) binding site is shown as residue 117–133, far removed from the XL site. (c) Cardiomyocytes were incubated with a peptide with the sequence 117–133, D-dimer, or scrambled peptide. D-dimer and the gamma (117–133) peptide resulted in significant decreases in fractional shortening (FS), whereas scrambled peptide had no significant effect. *,†$p < 0.05$ versus control.

Key messages

- Intracardiac intracellular adhesion molecule-1 (ICAM-1) and fibrinogen are increased as a result of systemic inflammation.
- Amino acid sequence 117–133 of the fibrinogen gamma chain is responsible for binding ICAM-1, functionally decreasing cardiomyocyte contractility.
- D-dimer contains the fibrinogen gamma chain and also decreases cardiomyocyte contractility.

Competing interests

The authors declare that they have no competing interests.

Authors' contributions

JHB drafted the manuscript. EHC performed the initial contractility measurements. EYD helped design the contractility experiments. CT performed the peptide experiments. RMB performed immunohistochemistry. GH designed the peptides. YW performed the animal work. KRW conceived of the study, participated in its design and coordination, and helped to draft the manuscript. All authors read and approved the final manuscript.

Acknowledgements

This work was supported by the Canadian Institutes of Health Research. KRW is a Michael Smith Foundation for Health Research (MSFHR) Distinguished Scholar. JHB is an IMPACT (Integrated and mentored pulmonary and cardiovascular training) postdoctoral fellow. RMB is an MSFHR postdoctoral fellow.

References

1. Van Eyk JE, Powers F, Law W, Larue C, Hodges RS, Solaro RJ: **Breakdown and release of myofilament proteins during ischemia and ischemia/reperfusion in rat hearts: identification of degradation products and effects on the pCa-force relation.** *Circ Res* 1998, **82**:261-271.
2. Reilly JM, Cunnion RE, Burch-Whitman C, Parker MM, Sheinhamer JH, Parrillo JE: **A circulating myocardial depressant substance is associated with cardiac dysfunction and peripheral hypoperfusion (lactic acidemia) in patients with septic shock.** *Chest* 1989, **95**:1072-1080.
3. Yano M, Ono K, Ohkusa T, Suetsugu M, Kohno M, Hisaoka T, Kobayashi S, Hisamatsu Y, Yamamoto T, Noguchi N, *et al.*: **Altered stoichiometry of FKBP12.6 versus ryanodine receptor as a cause of abnormal Ca(2+) leak through ryanodine receptor in heart failure.** *Circulation* 2000, **102**:2131-2136.
4. Lowe GD, Rumley A, McMahon AD, Ford I, O'Reilly DS, Packard CJ: **Interleukin-6, fibrin D-dimer, and coagulation factors VII and XIIa in prediction of coronary heart disease.** *Arterioscler Thromb Vasc Biol* 2004, **24**:1529-1534.
5. Lowe GD: **Circulating inflammatory markers and risks of cardiovascular and non-cardiovascular disease.** *J Thromb Haemost* 2005, **3**:1618-1627.
6. McDermott MM, Ferrucci L, Liu K, Criqui MH, Greenland P, Green D, Guralnik JM, Ridker PM, Taylor LM, Rifai N, *et al.*: **D-dimer and inflammatory markers as predictors of functional decline in men and women with and without peripheral arterial disease.** *J Am Geriatr Soc* 2005, **53**:1688-1696.
7. Heuer JG, Sharma GR, Gerlitz B, Zhang T, Bailey DL, Ding C, Berg DT, Perkins D, Stephens EJ, Holmes KC, *et al.*: **Evaluation of protein C and other biomarkers as predictors of mortality in a rat cecal ligation and puncture model of sepsis.** *Crit Care Med* 2004, **32**:1570-1578.
8. Sagastagoitia JD, Sáez Y, Vacas M, Narváez I, Sáez de Lafuente JP, Molinero E, Magro A, Lafita M, Santos M, Escobar A, *et al.*: **Association between inflammation, lipid and hemostatic factors in patients with stable angina.** *Thromb Res* 2007, **120**:53-59.
9. Davani EY, Dorscheid DR, Lee CH, van Breemen C, Walley KR: **Novel regulatory mechanism of cardiomyocyte contractility involving ICAM-1 and the cytoskeleton.** *Am J Physiol Heart Circ Physiol* 2004, **287**:H1013-1022.
10. Poon BY, Ward CA, Cooper CB, Giles WR, Burns AR, Kubes P: **Alpha(4)-integrin mediates neutrophil-induced free radical injury to cardiac myocytes.** *J Cell Biol* 2001, **152**:857-866.
11. Entman ML, Youker K, Shoji T, Kukielka G, Shappell SB, Taylor AA, Smith CW: **Neutrophil induced oxidative injury of cardiac myocytes. A compartmented system requiring CD11b/CD18-ICAM-1 adherence.** *J Clin Invest* 1992, **90**:1335-1345.
12. Raeburn CD, Calkins CM, Zimmerman MA, Song Y, Ao L, Banerjee A, Harken AH, Meng X: **ICAM-1 and VCAM-1 mediate endotoxemic myocardial dysfunction independent of neutrophil accumulation.** *Am J Physiol Regul Integr Comp Physiol* 2002, **283**:R477-486.
13. Davani EY, Boyd JH, Dorscheid DR, Wang Y, Meredith A, Chau E, Singhera GK, Walley KR: **Cardiac ICAM-1 mediates leukocyte-dependent decreased ventricular contractility in endotoxemic mice.** *Cardiovasc Res* 2006, **72**:134-142.
14. Landis RC, McDowall A, Holness CL, Littler AJ, Simmons DL, Hogg N: **Involvement of the "I" domain of LFA-1 in selective binding to ligands ICAM-1 and ICAM-3.** *J Cell Biol* 1994, **126**:529-537.
15. Staunton DE, Marlin SD, Stratowa C, Dustin ML, Springer TA: **Primary structure of ICAM-1 demonstrates interaction between members of the immunoglobulin and integrin supergene families.** *Cell* 1988, **52**:925-933.
16. Clayton A, Evans RA, Pettit E, Hallett M, Williams JD, Steadman R: **Cellular activation through the ligation of intercellular adhesion molecule-1.** *J Cell Sci* 1998, **111 (Pt 4)**:443-453.
17. Duperray A, Languino LR, Plescia J, McDowall A, Hogg N, Craig AG, Berendt AR, Altieri DC: **Molecular identification of a novel fibrinogen binding site on the first domain of ICAM-1 regulating leukocyte-endothelium bridging.** *J Biol Chem* 1997, **272**:435-441.
18. Languino LR, Plescia J, Duperray A, Brian AA, Plow EF, Geltosky JE, Altieri DC: **Fibrinogen mediates leukocyte adhesion to vascular endothelium through an ICAM-1-dependent pathway.** *Cell* 1993, **73**:1423-1434.
19. Languino LR, Duperray A, Joganic KJ, Fornaro M, Thornton GB, Altieri DC: **Regulation of leukocyte-endothelium interaction and leukocyte transendothelial migration by intercellular adhesion molecule 1-fibrinogen recognition.** *Proc Natl Acad Sci USA* 1995, **92**:1505-1509.
20. Sans E, Delachanal E, Duperray A: **Analysis of the roles of ICAM-1 in neutrophil transmigration using a reconstituted mammalian cell expression model: implication of ICAM-1 cytoplasmic domain and Rho-dependent signaling pathway.** *J Immunol* 2001, **166**:544-551.
21. Gardiner EE, D'Souza SE: **Sequences within fibrinogen and intercellular adhesion molecule-1 (ICAM-1) modulate signals required for mitogenesis.** *J Biol Chem* 1999, **274**:11930-11936.
22. Pluskota E, D'Souza SE: **Fibrinogen interactions with ICAM-1 (CD54) regulate endothelial cell survival.** *Eur J Biochem* 2000, **267**:4693-4704.
23. Parker JL: **Contractile function of heart muscle isolated from endotoxin-shocked guinea pigs and rats.** *Adv Shock Res* 1983, **9**:133-145.
24. Heneka MT, Loschmann PA, Osswald H: **Polymerized hemoglobin restores cardiovascular and kidney function in endotoxin-induced shock in the rat.** *J Clin Invest* 1997, **99**:47-54.
25. Nozawa T, Yasumura Y, Futaki S, Tanaka N, Uenishi M, Suga H: **Efficiency of energy transfer from pressure-volume area to external mechanical work increases with contractile state and decreases with afterload in the left ventricle of the anesthetized closed-chest dog.** *Circulation* 1988, **77**:1116-1124.
26. Kass DA, Maughan WL, Guo ZM, Kono A, Sunagawa K, Sagawa K: **Comparative influence of load versus inotropic states on indexes of ventricular contractility: experimental and theoretical analysis based on pressure-volume relationships.** *Circulation* 1987, **76**:1422-1436.
27. Walker JB, Nesheim ME: **The molecular weights, mass distribution, chain composition, and structure of soluble fibrin degradation products released from a fibrin clot perfused with plasmin.** *J Biol Chem* 1999, **274**:5201-5212.
28. Lindbom L: **Regulation of vascular permeability by neutrophils in acute inflammation.** *Chem Immunol Allergy* 2003, **83**:146-166.
29. Lominadze D, Tsakadze N, Sen U, Falcone JC, D'Souza SE: **Fibrinogen and fragment D-induced vascular constriction.** *Am J Physiol Heart Circ Physiol* 2005, **288**:H1257-1264.

hypertension, and attenuated the histological appearance of the lung damage, without an obvious protective effect on organ function and respiratory mechanics.

References

1. Otterbein L, *et al.*: *Nat Med* 2000, **6**:422-428.
2. Hoetzel A, *et al.*: *Antioxid Redox Signal* 2007, **9**:2013-2026.

P395

Endotoxemia induces an early differential metabolic response in the heart and liver as determined by metabolomic analysis

RM Bateman, M Ohmura, Y Nagahata, T Hishiki, M Suematsu
Keio University, Tokyo, Japan
Critical Care 2008, **12(Suppl 2)**:P395 (doi: 10.1186/cc6616)

Introduction Sepsis induces a hypermetabolic state and impairs energy metabolism. In this preliminary small animal study, we used recently developed metabolomics technology to test the hypothesis that metabolic shifts in glucose and amino acid metabolism in the heart and liver occur during the onset of endotoxemia.
Methods Sepsis was modeled in C57BL/6 mice via administration of lipopolysaccharide (LPS) (intraperitoneally, 40 mg/kg). Five hours post LPS, the left lobe of the liver and the heart were harvested. High-throughput capillary electrophoresis–mass spectrometry was used to identify and quantify metabolite levels based on their unique mass/charge ratio. The advantage of this metabolomics approach is that over 1,000 charged species can be detected in a single sample, generating a unique metabolic profile or readout.
Results Figure 1 shows relative changes in glucose and glycolytic metabolites, Kreb's cycle intermediates, NADH, ATP and amino acids between 5-hour LPS ($n = 2$) and control mice ($n = 2$). Metabolomic analysis suggested that endotoxemia caused an early increase in glucose metabolism in the heart, but a decrease in the liver. NADH levels increased in the liver, but not the heart, while ATP levels decreased in both the liver and the heart. Amino acid levels increased in the liver, with the exception of alanine and glycine, but were more variable in the heart.
Conclusions Five hours after LPS administration, we found differential glucose and amino acid metabolism in the heart and liver, indicating that profound shifts in metabolism occurred during the onset of endotoxemia.

P396

Noradrenaline for treatment of endotoxemic shock in pigs associated with improved hepatic mitochondrial respirati

T Regueira, S Djafarzadeh, PM Lepper, B Bänziger, S Brand J Takala, SM Jakob
Bern University Hospital (Inselspital), University of Bern, Switzerland
Critical Care 2008, **12(Suppl 2)**:P396 (doi: 10.1186/cc6617)

Introduction The optimal mean arterial blood pressure (MAP) sepsis resuscitation remains unclear. Growing evidence suggests mitochondrial dysfunction plays a role in the pathogenesis of sep induced organ failures. The aim of this study was to evaluate the e of progressively increasing levels of MAP, achieved by the us noradrenaline (NA) on liver mitochondrial function during sepsis.
Methods Thirteen anesthetized pigs received endot (*Escherichia coli* LPS B0111:B4, 0.4 μg/kg/hour until the m pulmonary arterial pressure reached 35 mmHg) and v subsequently randomized to placebo or NA administration for hours. The NA dose was adjusted every 2 hours to achieve mmHg increases in MAP up to 95 mmHg. Systemic (thermodilu and hepatosplanchnic blood flow (ultrasound Doppler) v measured at each step. At the end of the experiment, hep mitochondrial oxygen consumption (high-resolution respirom and citrate synthase activity (spectrophotometrically) were asses using the Oxygraph 2K (Oroboros Instruments, Innsbruck, Aus and DatLab 4.2 software for data acquisition and analysis.
Results The MAP, cardiac output and systemic DO_2 increase the NA group to 95 ± 7 mmHg (controls: 64 ± 3 mmHg), 8 3.1 l/min (controls: 5.7 ± 1.4 l/min), and 33 ± 8 ml/mi (controls: 17.6 ± 3.4 ml/min/kg; all $P < 0.05$). Systemic hepatosplanchnic VO_2 were not different between groups. Hep lactate uptake decreased significantly in both groups, but wit differences between the groups. At the end of the experiment, mitochondrial function in the NA group exhibited a signifi improvement in terms of maximal complex I-dependent r chondrial respiration (from 329 ± 83 to 587 ± 195 pmol/s/ and of respiratory control ratio for complex I (from 3.8 ± 1. 5.7 ± 0.5) and complex II (from 3.2 ± 0.5 to 3.9 ± 0.6; all $P < 0$ There were no differences in citrate synthase activity betweer groups (13.9 ± 3 vs 16.8 ± 4 μmol/min/mg).

Figure 1 (abstract P395)

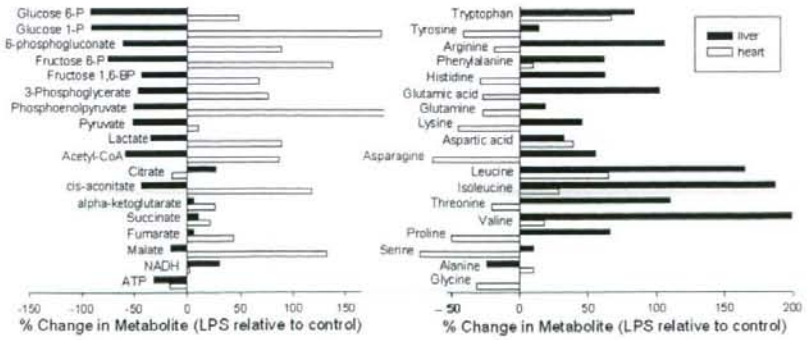

Metabolic profiles for glucose (left) and amino acid (right) metabolism.

Endotoxemia induces a differential metabolic response in the heart and liver as determined by metabolomic analysis

Ryon M Bateman[1], Reiichiro Obata[1], Yoshiko Nagahata[1], Mitsuyo Ohmura[1], Takako Hishiki[1], Makoto Suematsu[1]. Department of Biochemistry and Integrative Medical Biology, School of Medicine, Keio University, 160-8582, Tokyo, Japan

(characters 339/400)

The systemic inflammatory response to bacterial infection (sepsis) alters microvascular and mitochondrial function; yet, little is known about effects on metabolism. The objective was to determine how intermediary carbohydrate metabolism changes during the onset of sepsis. C57bl/6 mice (30-35g) were injected intraperitoneally with lipopolysaccharide (LPS, 40mg/kg). Six hours post LPS, C13-pyruvate (a key intermediate metabolite) was administered subcutaneously. At 20,40 and 60 minutes, heart and liver tissues were harvested and stored at -80C. Capillary electrophoresis - mass spectrometry (CE-MS) quantified metabolic intermediates. Labeled metabolites were normalized to non-labeled metabolite levels. Pyruvate was preferentially metabolized by the heart, but uptake was delayed in both liver and heart relative to control. Lactate, TCA intermediates (citrate, a-ketoglutarate, malate), G1P and UDP-glucose increased in the endotoxemic heart. By contrast, glutamate and B-hydroxybutyrate increased in endotoxemic liver. Fluxome analysis of pyruvate metabolism suggests the endotoxemic heart stores glucose, while the liver generates alternative energy sources. Funding source, MEXT Japan.

 Articles in PresS. Am J Physiol Renal Physiol (October 29, 2008). doi:10.1152/ajprenal.00013.2008

CD36 is one of important receptors promoting renal tubular injury by advanced oxidation protein products

Yasunori Iwao[1], Keisuke Nakajou[1], Ryoji Nagai[2], Kenichiro Kitamura[3], Makoto Anraku[1], Toru Maruyama[1], Masaki Otagiri[1*]

[1]Department of Biopharmaceutics, Graduate School of Pharmaceutical Sciences, Kumamoto University, Kumamoto, Japan

[2] Department of Medical Biochemistry, Graduate School of Medical Sciences, Kumamoto University, Kumamoto, Japan

[3] Department of Nephrology, Graduate School of Medical Sciences, Kumamoto University, Kumamoto, Japan

Running head:

CD36 is involved in renal tubular injury caused by AOPPs

Copyright © 2008 by the American Physiological Society.

*Address correspondence to:

Masaki Otagiri, Ph.D.

Professor

Department of Biopharmaceutics,

Graduate School of Pharmaceutical Sciences,

Kumamoto University

5-1 Oe-honmachi, Kumamoto 862-0973, Japan

Phone: +81-96-371-4150

Fax: +81-96-362-7690

E-mail: otagirim@gpo.kumamoto-u.ac.jp

ABSTRACT

Chronic accumulation of plasma advanced oxidation protein products (AOPPs) promotes renal fibrosis. However, the mechanism at cellular level has not been clarified. In the present study, endocytic assay of human proximal tubular cells (HK-2 cells) demonstrated that AOPPs-HSA (*in vitro* preparations of chloramine-T modified human serum albumin (HSA)) were significantly endocytosed in a dose-dependent manner at a higher level than HSA. The expression of CD36, a transmembrane protein of the class B scavenger receptor, in HK-2 cells was confirmed in the immunoblot analysis. In a cellular assay using over-expressing human CD36 in CHO cells, AOPPs-HSA were significantly endocytosed by CD36-CHO cells, but not by mock-CHO cells. Furthermore, the endocytic association and degradation of AOPPs-HSA by HK-2 cells was significantly inhibited by anti-CD36 antibody treatment, suggesting that CD36 is partly involved in the uptake of AOPPs-HSA by HK-2 cells. AOPPs-HSA upregulated the expression of CD36 in a dose-dependent manner. In addition, AOPPs-HSA upregulated the generation of intracellular reactive oxygen species and the secretion of TGF-β1 in HK-2 cells, whereas anti-CD36 antibody neutralize the upregulation of TGF-β1. These results suggest that AOPPs-HSA may cause renal tubular injury via the CD36 pathway.

KEY WORDS: advanced oxidation protein products; renal tubular injury; CD36; endocytosis; TGF-β1

ABBREVIATIONS: AOPP, advanced oxidation protein products; HSA, human serum albumin; CKD, chronic kidney disease; ROS, reactive oxygen species; PKC, protein kinase C;

INTRODUCTION

Proteinuria is a prominent feature of many renal diseases. It is a consequence of glomerular capillary walls breakdown, causing abnormal transglomerular passage of plasma protein. Excessive plasma proteins can gain access to the proximal tubular cells (PTC), causing tubulointerstitial inflammation, tubular atrophy, and tubulointerstitial fibrosis (2, 41). The most prevalent protein in the urine of nephritic patients is human serum albumin (HSA). Several authors have postulated that excessive filtration of HSA into proximal tubules may have a detrimental effect on tubulointerstitial function (18, 44). In *in vitro* experiments, albumin stimulates various intracellular signaling pathways in PTC and induces them to produce various chemoattractants and proinflammatory and profibrotic cytokines (4, 11, 12, 46, 52). Some authors have also demonstrated a pro-apoptotic effect of albumin in cultured PTC (14, 21). Thus, albumin is one of the major mediators of renal tubulointerstitial disease.

HSA is the most abundant plasma protein and serves as a carrier of endogenous and exogenous compounds (39). In addition, HSA is quite vulnerable to reactive oxygen species (ROS) (9). In chronic kidney disease (CKD) oxidative stress is increased, as there is an imbalance between excessive generation of oxidant compounds and insufficient anti-oxidant defense mechanisms. This results in the generation of large amounts of ROS, such as $O_2^{\bullet-}$, H_2O_2 and HOCl, by activation of neutrophils. In particular, HOCl, which is a powerful oxidizing agent, reacts with a wide variety of biological molecules, such as DNA, amino acids, peptides and proteins (1, 40, 47). Recently, Witko-Sarsat et al. reported the presence of elevated levels of advanced oxidation protein products (AOPPs)

in the plasma of uremia (48) and Capeillere-Blandin et al. identified albumin as the main AOPPs in plasma (5). Furthermore, plasma concentration of AOPPs was closely correlated with the levels of dityrosine, a hallmark of oxidized protein, and pentosidine, a marker of protein glycation closely related to oxidative stress (19). Thus, AOPPs might be formed during oxidative stress by the reaction of plasma albumin with chlorinated oxidants and considered novel markers of oxidant-mediated protein damage (48).

A more recent finding is that AOPPs are highly correlated with carotid intima media thickness (13) and may even be related to atherosclerotic cardiovascular events (10). Chronic administration of AOPPs accelerated atherosclerosis in a hyperlipidemic rabbit model (29). A clinical study revealed a close relationship between levels of AOPPs and serum markers of monocyte activation (49). These data suggest that these oxidized proteins contribute to the inflammatory processes associated with several diseases. Based on this information, we hypothesized that a large amount of plasma AOPPs may access proximal tubular cells across the glomerulus and cause proximal tubular cell injury, such as that caused by HSA. Recently, Li et al. showed that treatment with AOPPs-RSA enhanced AOPPs levels in plasma and renal tissue and upregulated expression of monocyte chemoattractant protein-1 and TGF-β1 in the renal cortex, demonstrating that chronic accumulation of AOPPs promotes renal fibrosis (26). However, the underlying mechanisms of induced progressive renal damage by AOPPs at the cellular level remain largely unresolved.

In the present study, chloramine-T (HOCl analog) was used to prepare AOPPs-HSA. Chloramines are primarily produced by HOCl reactions (43). Because chloramines retain the oxidizing equivalents of HOCl and are longer-lived than HOCl (38, 47), chloramines are one of the important oxidants involved in the progression of CKD. Therefore, we examined the mechanisms of AOPPs-HSA and the detrimental effects induced by AOPPs-HSA in HK-2 cells (*in vitro* model as PTC).

EXPERIMENTAL PROCEDURES

Chemicals. HSA was donated by the Chemo-Sera-Therapeutic Research Institute (Kumamoto, Japan). BSA (fraction V) was purchased from Wako Pure Chemical Industries, Ltd. (Osaka, Japan). Chloramine T and protease inhibitor cocktail were purchased from Nacalai Tesque (Kyoto, Japan). Keratinocyte-SFM and Epidermal Growth Factor (EGF) were purchased from Gibco Life Technologies. Bovine Pituitary Extract was purchased from Kurabo. Dulbecco's modified Eagle's medium (DMEM) was obtained from Sigma Chemical Co. (St. Louis, MO). Penicillin G (1650 IU/mg), streptomycin sulfate (750 IU/mg), G418 and Ham's F-12 medium were purchased from Life Technologies, Inc. $Na^{125}I$ (3.7 GBq/ml in NaOH) was purchased from Amersham Pharmarcia Biotech (Little Chalfont, Bucks., U.K.). Goat anti-CD36 polyclonal antibody (L-17), Goat anti-actin polyclonal antibody (I-19) and HRP-rabbit anti-goat IgG (H+L) were purchased from Santa Cruz Biotechnology. Mouse anti-human CD36 monoclonal antibody (FA6-152) was purchased from Immunotech. Humanized mouse anti-human LOX-1 monoclonal antibody (JTX92) was donated by Dr. T. Sawamura (National Cardiovascular Center Research Institute, Osaka, Japan.). All reagents used were of the highest grade available from commercial sources.

AOPPs-HSA preparation and determination. Fraction V HSA (96% pure) was defatted using the charcoal procedure described by Chen (6), deionized, freeze-dried and then stored at -20°C until used. AOPPs-HSA was prepared *in vitro* as described previously (22). Briefly, HSA (300 μM) was incubated for 1 hr in phosphate buffer (pH 8.0) at 37°C in an oxygen-saturated solution containing 100 mM chloramine-T, an HOCl

analogue. After incubation, the oxidation reactions were stopped by extensive dialysis of solutions against water. The control involved incubating HSA dissolved in buffer alone, and in all cases the proteins were stored at −20°C until used. The endotoxin levels in HSA and AOPPs-HSA were measured with the Limulus Amoebocyte lysate test (the endospecy test) and were found to be below 0.072 ng/mg protein in HSA and 0.095 ng/mg protein in AOPPs-HSA. Since Valencia et al. demonstrated that low levels of endotoxin (below 0.2 ng/mg protein) did not show any effects on the induction of cellular responses (45), we used those AOPPs-HSA preparations in the present study. The content of AOPPs, which was thought as a useful oxidative stress marker, was determined as described previously (49). Briefly, 200 μL of samples were placed in a 96-well microtiter plate (Becton Dickinson Labware, Lincoln Park, NJ) and mixed with 20 μL of acetic acid. In standard wells, 10 μL of 1.16 mol/L potassium iodide was added to 200 μL of chloramine-T solution, followed by 20μL of acetic acid. The absorbance of the reaction mixture at 340 nm was read immediately in a microplate reader. The contents of AOPPs in our AOPPs-HSA and HSA samples (1.34 mg/mL solutions) were 244.3 ± 12.3 μM and 10.3 ± 6.3 μM, respectively. Since we used 0.0025 - 5 mg/mL of AOPPs-HSA or HSA throughout the present study, the ranges of the AOPPs content in AOPPs-HSA and HSA were 0.46 - 911.5 μM and 0.019 - 38.5 μM, respectively. Dityrosine content, which is also a useful oxidative stress marker, of AOPPs-HSA was also significantly greater than that of HSA (0.7 ± 0.11 vs. 0.32 ± 0.13 nmol dityrosine per mg protein; $p < 0.01$). The contents of AOPPs and dityrosine in the plasma of hemodialysis patients are reported as 267.5 ± 16.5 μM and 1.03 ± 0.12 nmol dityrosine per mg protein, respectively (48), thus indicating that the degree of modification of our AOPPs-HSA preparation is

comparatively similar to that of AOPPs and dityrosine levels in the plasma of hemodialysis patients. To determine whether the AOPPs-HSA contained advanced glycation end products (AGE), we measured the content of N^{ε}-(carboxylmethyl)lysine (CML), pyrraline, pentosidine and imidazolone in both AOPPs-HSA and unmodified HSA by enzyme-linked immunosorbent assay (ELISA), as described elsewhere (32). Briefly, each well of a 96-well microtiter plate was coated with 100 μL of the sample to be tested in 50 mM sodium carbonate buffer (pH 9.6). Each well was then blocked with 0.5% gelatin, and washed 3 times with PBS containing 0.05% Tween 20 (washing buffer). The wells were incubated for 1 hr with each monoclonal antibody against these AGE structures dissolved in washing buffer. The wells were then washed with washing buffer 3 times, incubated with a horseradish peroxidase (HRP)-conjugated antimouse IgG antibody, and finally incubated with 1,2-phenylenediamine dihydrochloride. The reaction was terminated by the addition of 0.1 mL of 1.0 M sulfuric acid, and the absorbance at 492 nm was read on a micro-ELISA plate reader. As a result, there were no significant differences in the content of AGE structures between AOPPs-HSA and unmodified HSA. In addition, agarose gel electrophoresis was performed to examine whether there was unmodified HSA in AOPPs-HSA using the Universal Gel/8 electrophoresis kit (Ciba-Corning, Tokyo), followed by staining with Coomassie brilliant blue (33). As a result, the electrophoretic mobility of the AOPPs-HSA toward the anode was higher than that of unmodified HSA and there was no unmodified HSA in the AOPPs-HSA (data not shown).

Protein labeling with ^{125}I. AOPPs-HSA and HSA were labeled with ^{125}I by Iodo-Gen (Pierce), as previously described (35). A solution containing 10 μL of $Na^{125}I$ solution and 0.5 mg of proteins in 0.2 mL of 0.1 M sodium phosphate buffer (pH 7.4) in an Iodo-Gen-adhered test tube was incubated for 30 min at room temperature. Unreacted $Na^{125}I$ was removed by adding the solution to a PD-10 column followed by elution with PBS. The ^{125}I-labeled fractions were combined on the basis of their radioactivity, as determined with a well counter. The specific activities of HSA and AOPPs-HSA were 400 and 350 cpm/ng protein, respectively.

Cell culture of HK-2. The immortalized human proximal tubular cell line HK-2 (ATCC, Manassas, VA) was cultured at 37°C in 5% CO_2 in keratinocyte serum-free medium (K-SFM), supplemented with 5 ng/ml human recombinant epidermal growth factor and 0.05 μg/ml bovine pituitary extract. HK-2 cells were seeded to tissue culture flasks (greiner bio-one, Germany) and further grown to confluence until cellular assay.

Cell culture and isolation of a transfected cell line (CD36-CHO cells and mock-CHO cells). The cDNA of human CD36 was amplified from a human placenta cDNA library by polymerase chain reaction using the primers as described previously (37). The amplified human CD36 cDNA was transfected into Chinese hamster ovary (CHO)-K1 cells by the electroporation method. CD36-CHO cells were selected and maintained as described previously (37).